



Deposited via The University of Leeds.

White Rose Research Online URL for this paper:

<https://eprints.whiterose.ac.uk/id/eprint/43317/>

Article:

Saunders, RW, Forster, PM and Plane, JMC (2007) Potential climatic effects of meteoric smoke in the Earth's paleo-atmosphere. *Geophysical Research Letters*, 34 (16). ISSN: 0094-8276

<https://doi.org/10.1029/2007GL029648>

Reuse

See Attached

Takedown

If you consider content in White Rose Research Online to be in breach of UK law, please notify us by emailing eprints@whiterose.ac.uk including the URL of the record and the reason for the withdrawal request.

Potential climatic effects of meteoric smoke in the Earth's paleo-atmosphere

Russell W. Saunders,¹ Piers M. Forster,² and John M. C. Plane¹

Received 12 February 2007; revised 4 July 2007; accepted 19 July 2007; published 16 August 2007.

[1] Modelling of the growth of meteoric smoke in the Earth's atmosphere, by assuming the formation of either simple spherical (compact) particles or, more realistically, fractal (porous) aggregates, highlights important differences in the predicted atmospheric size distributions as a function of altitude. The calculated UV extinction and direct radiative forcing (DRF) of these types of particles is also quite different. It is shown that, with regard to (a), forming a UV barrier before the presence of significant ozone levels in the atmosphere and (b), triggering 'snowball Earth' glaciations by negative DRF, fractal smoke particles are unlikely to have been important even if the flux of interplanetary dust into the atmosphere was 3 orders of magnitude higher than the present day. However, if these particles are effective ice nuclei, then subsequent indirect forcing through ice cloud formation could have made a more significant contribution to the onset of ancient glaciation episodes. **Citation:** Saunders, R. W., P. M. Forster, and J. M. C. Plane (2007), Potential climatic effects of meteoric smoke in the Earth's paleo-atmosphere, *Geophys. Res. Lett.*, 34, L16801, doi:10.1029/2007GL029648.

1. Introduction

[2] Meteoric smoke particles are present in the atmosphere as a result of the condensation of the metal- and silicon-containing molecules produced by meteoric ablation in the upper mesosphere and lower thermosphere. These species are thought to play an important role in a number of atmospheric processes [Plane, 2003]. To date, modelling studies of the vertical distribution of these smoke particles in the atmosphere have assumed they are spherical in shape and compact in structure [e.g., Hunten et al., 1980; Gabrielli et al., 2004].

[3] However, there are several pieces of evidence which indicate that the particles are much more likely to be fractal-like and have porous or 'fluffy' structures. Firstly, interplanetary dust particles (IDPs) sampled from the stratosphere often display an aggregated, non-spherical form [Rietmeijer, 2002]. This type of particle, as is likely the case with meteoric smoke, originates from the condensation of metal oxides and silicates [Henning, 1998]. Secondly, the characteristics of a scattering layer which was observed by lidar to descend through the stratosphere [Gerding et al., 2003] were best explained in terms of non-spherical particles of meteoric composition. Finally, we have recently conducted a laboratory study to generate analogues of meteoric smoke

in a photo-chemical flow reactor [Saunders and Plane, 2006]. These experiments produced extended particle aggregates with amorphous, porous structures and mineral compositions such as hematite (Fe_2O_3) and fayalite (Fe_2SiO_4). Modelling of the growth kinetics of these particles showed that the rates of aggregation were enhanced by long-range inter-particle magnetic dipole interactions, which are most likely also responsible for the extended structures.

[4] In this paper we discuss the results from a 1-dimensional model developed to describe the growth and gravitational sedimentation of fractal, magnetic particles in the Earth's atmosphere. The size- and height-resolved number concentrations predicted from the model are then used to estimate the optical extinction resulting from meteoric smoke, as a function of the IDP flux entering the atmosphere. Evidence for episodic enhancements in the flux level comes from geochemical analysis of cosmic tracers such as osmium, iridium, ^3He and ^{21}Ne in ancient sediment strata [Schmitz et al., 1997; Bodiselitsch et al., 2005; Heck et al., 2004].

[5] We then use the smoke model to explore two potential roles for meteoric smoke particles in the early Earth's atmosphere. The first role was as a UV barrier prior to O_2 , and hence O_3 , rising above the very low levels present in the paleo-atmosphere (up to ~ 2.3 billion years before present (BP)). Such species are required to be strongly absorbing at UV wavelengths ($\lambda < 350$ nm) while largely transparent in the visible region, allowing surface temperatures to have been maintained at a sufficiently high level for O_2 -producing organisms to have established and thrived.

[6] A second possible role for meteoric smoke was in the initiation of the two global glaciation periods which occurred during the Neo-Proterozoic era (~ 1000 – 540 million years BP)—the 'snowball Earth' scenario [Kirschvink, 1992; Hoffman et al., 1998]. The mechanism originally suggested for the onset of these widespread glaciations is the draw-down of CO_2 from the atmosphere due to 'super-continent' break-up. More recently, a study by Pavlov et al. [2005] proposed that increased interstellar dust concentrations in the atmosphere, due to the Earth's passage through a giant molecular cloud, could have resulted in sufficiently high levels of light extinction (i.e., negative radiative forcing) to have triggered the onset of global ice coverage. It is this hypothesis that we examine further here.

2. Particle Growth: Spherical Versus Fractal Morphology

[7] A 1-D particle microphysics model was used to determine the growth and vertical distribution of meteoric smoke in the Earth's atmosphere from 110 km down to 20 km, with a vertical resolution of 1 km. Present-day

¹School of Chemistry, University of Leeds, Leeds, UK.

²School of Earth and Environment, University of Leeds, Leeds, UK.

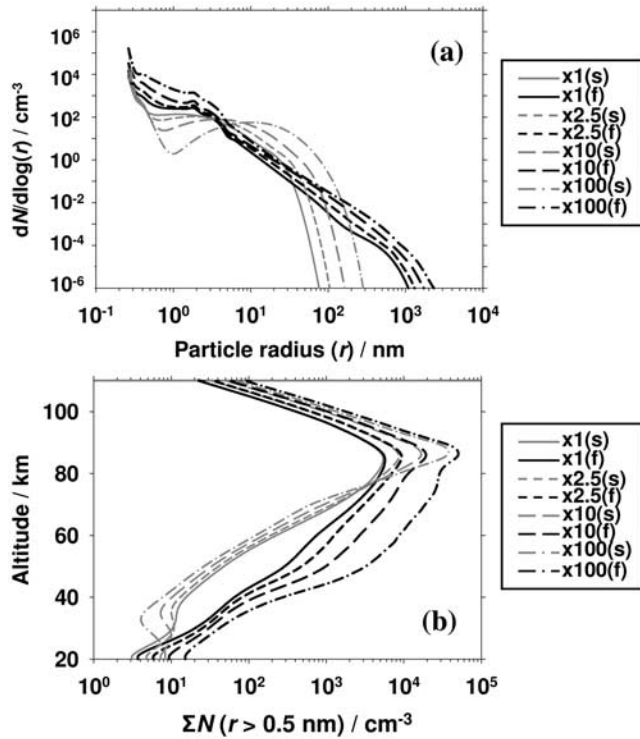


Figure 1. (a) Modelled size distributions of meteoric smoke particles at 70 km altitude assuming either spherical (s) or fractal (f) growth, at different dust fluxes where ‘ $\times 1$ ’ is equivalent to the present day value of 44 tonnes per day, and (b) height resolved particle concentration profiles for the same scenarios as in Figure 1a.

temperature, density and vertical eddy diffusion coefficient (K_{zz}) profiles (March, 70°N) were taken from the SOCRATES model [Huang *et al.*, 1998], and were used for all model runs. K_{zz} varied from a maximum of $52 \text{ m}^2 \text{ s}^{-1}$ at 101 km to a minimum of $0.4 \text{ m}^2 \text{ s}^{-1}$ at altitudes below 45 km. Though the structure and circulation of the pre O_2 -rich atmosphere was undoubtedly different from the present day, the effect on the meteoric smoke column abundance, which is our concern here, was probably minor.

[8] The input ablation profile, which peaks at 92 km, was taken from Plane [2004] for an IDP flux of 44 tonnes per day (t d^{-1}) as used in the original meteoric smoke paper of Hunten *et al.* [1980]. For this study the profile is simply scaled proportional to this IDP flux. Particle composition was chosen as fayalite (Fe_2SiO_4 , molecular mass = 204 amu) with a bulk density (ρ_b) of 4400 kg m^{-3} , giving a molecular radius of 0.26 nm. We do not expect that the composition of meteoric smoke would have been very different in the ancient atmosphere, which would still have been N_2 -dominated with sufficient traces of O_2 and O_3 to oxidise the Fe and Si atoms (produced by meteoric ablation) to form FeO_3 and SiO_2 species, the likely precursors of fayalite [Saunders and Plane, 2006].

[9] Gravitational sedimentation was parameterised within the model using Stokes Law, modified for the slip-flow regime [Jacobson, 2005; Kasten, 1968]. For fractal particles, prolate (needle-like) morphology was assumed with a chosen aspect ratio of 5:1, and sedimentation velocities calculated at volume-equivalent radii and using size-

dependent fractal particle densities. These are determined in the model from the parameters of fractal dimension (D_f) and primary particle radius (r_0), which are used to characterise the fractal structures [Jacobson, 2005], and the bulk density of the chosen material. Conservation of total particle mass was verified for all model runs. Particle residence times were ~ 60 days in the mesosphere and ~ 1500 days in the stratosphere. Particle number distributions were determined for a range of dust fluxes covering up to 3 orders of magnitude above the base level of 44 t d^{-1} . Henceforth, we refer to this value as the present day flux (PDF).

[10] Figure 1a shows the predicted particle size distributions at a height of 70 km, obtained from $\times 1$, $\times 2.5$, $\times 10$ and $\times 100$ PDF for scenarios of spherical ($D_f = 3$) particles (denoted by ‘s’), and fractal particles (‘f’) with D_f , r_0 , and the degree of magnetic dipole alignment within the particles set at 1.75, 4.2 nm and 0.24 respectively, in accord with the results of our laboratory study [Saunders and Plane, 2006].

[11] At $\times 1$ PDF, the fractal treatment results in enhancements to the predicted particle number concentrations for $r > 35$ nm at the expense of particles at $r_0 < r < 35$ nm. This is due to the larger collision kernels for magnetically interacting particles (compared with non-magnetic or Brownian kernels) for $r > r_0$, which lead to extended fractal structures. At larger IDP fluxes, this trend is repeated with higher concentrations of particles at larger sizes within each distribution compared with the respective spherical particle distributions at $r > 52$ nm ($\times 2.5$ PDF), > 77 nm ($\times 10$ PDF) and > 139 nm ($\times 100$ PDF).

[12] The height-resolved particle number concentrations ($r > 0.5$ nm) are shown in Figure 1b for the same scenarios as in Figure 1a. All spherical and fractal particle distributions peak at ~ 85 km. However, for the fractal runs there is a distinct enhancement in the particle concentrations below this peak which becomes increasingly pronounced at the larger IDP fluxes. The reason for this enhancement is that the larger particles coagulate with each other much more quickly than with the small particles, so that a large population of small particles ($r < r_0$) is “left behind” as the size distribution evolves, leading to a higher total particle number than in the spherical case.

[13] Our model does not take into account any effects associated with the charging of aerosol particles in the atmosphere above ~ 75 km, which could be significant [see Rapp and Lübken, 2001]. There are two reasons we do not treat particle charging: first, there is current uncertainty regarding the fraction (and sign) of charged aerosols, and hence the likely impact on coagulation rates. Second, the collision kernels for charge-induced dipole interactions between charged and uncharged particles are likely to be much less significant in comparison with the kernels determined for the magnetic dipole interactions of iron-containing smoke particles [Saunders and Plane, 2006].

3. Light Extinction by Meteoric Smoke Particles

[14] Refractive index data ($400 \text{ nm} < \lambda < 2 \text{ }\mu\text{m}$) for crystalline fayalite was used to determine the resultant light extinction expected from the modelled smoke particle size distributions. At wavelengths below 400 nm, the real and imaginary refractive indices were extrapolated in line with

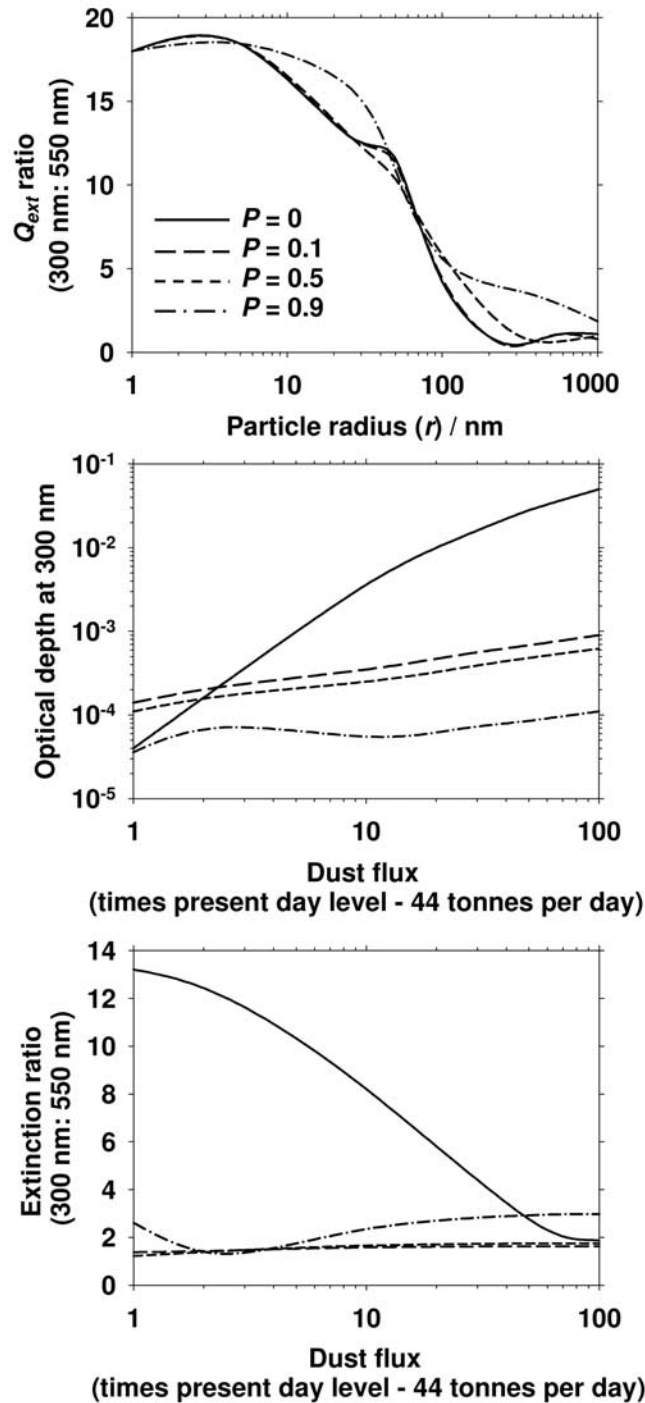


Figure 2. (top) Variation with particle size of the UV-visible extinction efficiency ratio for meteoric smoke particles of both spherical and fractal morphology, with fayalite composition. (middle) Smoke particle optical depth (extinction) at 300 nm as a function of initial dust flux into the atmosphere. (bottom) Change in integrated particle extinction ratio with dust flux. P is the average particle porosity at $r > r_0$ (4.2 nm) with $P = 0$ corresponding to spherical, compact particles. In the top panel, the $P = 0$ and $P = 0.1$ lines are indistinguishable from each other.

the respective trends for olivine, for which values are reported for the near-UV wavelength region in the same database [Jäger *et al.*, 2003]. Extinction efficiencies (Q_{ext}) were determined using Rayleigh theory for very small particles ($r \leq r_0$), and Mie theory for larger particle sizes. Fractal particles were treated as ‘equivalent porous spheres’, composed of solid, silicate matrix with small vacuum inclusions (size $\ll \lambda$). Maxwell-Garnett effective medium theory [Ossenkopf, 1991] was then used to determine particle refractive indices over a range of average porosities, where porosity (P) is defined as the fraction of vacuum within the particle structure, and optical parameters calculated at volume-equivalent radii for $r > r_0$.

4. UV Screening Potential of Meteoric Smoke

[15] To assess the potential for meteoric smoke particles to act as a UV barrier, we calculated the Q_{ext} ratio for fayalite particles at 300 nm and 550 nm. This ratio is plotted in Figure 2 (top) as a function of r , for the cases of spherical particles ($P = 0$) and fractal particles ($P = 0.1, 0.5$ and 0.9).

[16] In all cases, this ratio is greater than 10 for $r < 50$ nm, and converges to ~ 1 at the largest sizes considered. Over a range of IDP fluxes up to $\times 100$ PDF, the size- and height-integrated extinction ratio (Figure 2, bottom) only exceeds 10 for the case of spherical particles when the flux is less than $\times 5$ PDF (extinction values at 300 nm are shown in Figure 2 (middle)). At larger IDP fluxes, the extinction ratio steadily decreases because of the increasing number concentrations of particles with $r > 50$ nm (see Figure 1a), for which extinction at visible wavelengths becomes increasingly dominant compared with smaller particles. In the fractal case, the extinction ratio shows a much flatter dependence on the IDP flux, with a maximum value of 3.0 at $\times 100$ PDF for the highest particle porosity considered ($P = 0.9$). At all fluxes, the low ratios are due to a combination of lower refractive indices (for $P > 0$) for fractal particles compared with spherical particles of equivalent sizes, and higher concentrations of larger particles at sizes which again result in increased extinction in the visible.

[17] Determination of surface UV radiation levels [Forster, 1995] for the scenario of an early Earth atmosphere (1% O_2) with and without meteoric smoke present, indicates that, at a solar zenith angle of 0° , the presence of fractal particles will have a negligible impact on UVC ($\lambda < 280$ nm) and UVB ($\lambda = 280$ – 320 nm) levels even at the highest fluxes considered. This is consistent with the trends observed in Figure 2 - top (low Q_{ext} ratio at large r) and Figure 2 - bottom (low integrated extinction ratios at all fluxes). For comparison, spherical smoke particles are predicted to reduce UVC by $\sim 0.5\%$ and have a negligible impact on UVB at $\times 100$ PDF, whilst at $\times 500$ PDF, smoke particles will reduce UVC levels by 6% and UVB by 5%. In conclusion, our analysis indicates at best a minor supporting role (along with other potential aerosol species) for meteoric smoke particles as an early UV barrier.

5. Potential for Inducing Glaciation Episodes

[18] According to Pavlov *et al.* [2005], a critical direct radiative forcing (DRF) level of $(-)$ 9.3 W m^{-2} would have

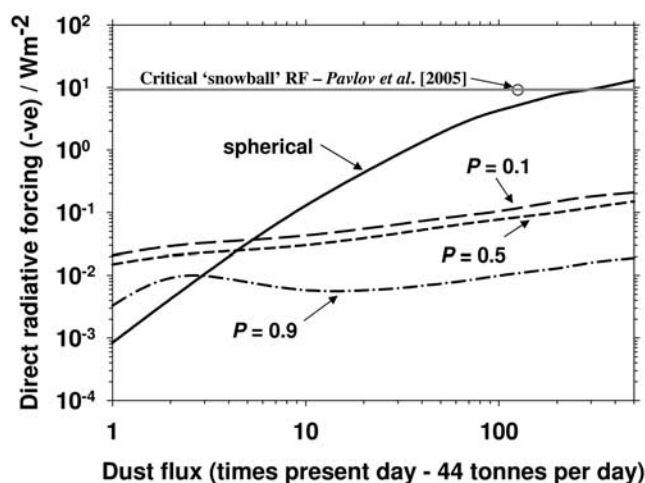


Figure 3. Radiative forcing levels resulting from fayalite smoke particle light extinction, for varying initial material flux rates to the Earth's atmosphere. Values are shown for spherical particles and for fractal particles with different average porosities as indicated. Also shown is the critical level of $(-)$ 9.3 Wm^{-2} calculated by Pavlov *et al.* [2005] – see text.

caused global-scale glaciation (assuming an initial present-day surface temperature and ice coverage). In their study, they assumed that interstellar dust would be in the form of spherical particles with a mixed silicate and carbon composition, and found that a dust flux of $\sim 5500 \text{ t d}^{-1}$ (i.e. $\sim \times 125$ PDF) would produce this critical RF level. For comparison, our Figure 3 shows the total DRF values determined from the smoke particle absorption and scattering depths, integrated from $200 \text{ nm} - 2 \text{ }\mu\text{m}$ and weighted to the present-day solar flux (top of atmosphere) over this wavelength range.

[19] These values were calculated by assuming a uniform, global distribution of the meteoric smoke and modifying the Chylek and Wong [1995] treatment to account for the aerosol being above the tropopause, by making the absorption term an additional negative forcing. We find that the critical RF level is reached with an IDP flux of $\sim \times 250$ PDF for the case of spherical meteoric smoke particles i.e., a flux that is about twice as large as found by Pavlov *et al.* [2005]. This difference appears to be due to their assumption of a pre-formed size distribution of particles which are then allowed to grow through coagulation, whereas in our model, particles grow from individual molecules of fayalite [Saunders and Plane, 2006]. The fractal growth and particle porosity treatments result in enhanced extinction and DRF at less than $\times 5$ PDF levels, whereas for higher fluxes and increasing average P values, the radiative forcing is predicted to fall significantly below that from spherical smoke particles. However, we should qualify this discussion of the DRF contributions resulting from meteoric smoke particles by repeating the observation made by Pavlov *et al.* [2005] that the calculated forcing values almost certainly represent lower limits to the total (direct + indirect) forcing due to refractory aerosol in the atmosphere. The ability of meteoric smoke particles to act as sites for the heterogeneous condensation and freezing of

water vapour has been studied in the laboratory [Bigg and Giutronich, 1967]. This work found that, per gram of meteoritic material, fluffy (non-spherical) particles were more efficient condensation nuclei compared with compact (spherical) particles. However, their nucleating efficiency has not been studied under realistic upper atmospheric conditions, in spite of the fact that they have long been proposed as condensation nuclei for NLCs in the upper mesosphere [Rapp and Thomas, 2006, and references therein].

[20] If an increase in the IDP flux was accompanied by a large increase in the flux of interstellar H_2 into the atmosphere, the resulting increase of H_2O [Yabushita and Allen, 1989] and hence ice cloud formation [McKay and Thomas, 1978] could have lead to a significant increase in albedo. We note that the predicted height-resolved particle concentrations (Figure 1b) in the mesosphere are significantly higher (e.g. by ~ 2 orders of magnitude at 60 km for $\times 100$ PDF) when fractal growth occurs. The ice nucleation potential for meteoric smoke is likely to be enhanced in the case of porous fractal aggregates due to their larger surface area-to-volume ratios in comparison with volume-equivalent spherical, compact particles. Hence, this potential is likely to be greater at high IDP fluxes which result in higher concentrations of such larger extended particle aggregates. In addition, meteoric smoke could also exert an indirect effect in the lower atmosphere. The particles are thought to be transported via meridional circulation in the mesosphere to the winter pole, and then descend into the lower stratosphere inside the polar vortex [Gabielli *et al.*, 2004; Curtius *et al.*, 2005], where they may impact on polar stratospheric cloud formation [Cziczo *et al.*, 2001]. The particles probably then enter the troposphere through mid-latitude tropopause folding. If the IDP flux were large enough, then smoke particles could increase the ice nucleus population, promoting increased cirrus cloud formation and modifying cloud optical properties, thus leading to an increase in the indirect forcing contribution.

6. Conclusions

[21] Our model of meteoric smoke formation, growth and vertical transport shows that particle concentrations at larger sizes are enhanced in the middle atmosphere when the particles have a fractal (porous) structure compared with spherical (compact) particles. One consequence of this is that the optical extinction ratio (UVB: visible) is predicted to be less than 2.0 for IDP fluxes from present day levels (44 t d^{-1}) up to 3 orders of magnitude above this level for realistic particle porosity values ($P < 0.9$). This trend indicates that any possible role for meteoric smoke as a UV barrier in the Earth's paleo-atmosphere is significantly reduced when non-spherical particle growth is accounted for. Even during periods of elevated IDP flux to the atmosphere, likely to have occurred in the Earth's past, we find that the direct radiative forcing due to fractal smoke particles would be much lower in comparison with that from spherical particles, and would be insufficient to have triggered snowball Earth glaciations.

[22] **Acknowledgments.** This work was supported by a fellowship from the University of Leeds (for RWS) and funding from the UK Natural Environment Research Council.

References

- Bigg, E. K., and J. Giutronich (1967), Ice nucleating properties of meteoritic material, *J. Atmos. Sci.*, *24*, 46–49.
- Bodiselsch, B., C. Koeberl, S. Master, and W. U. Reimold (2005), Estimating duration and intensity of Neoproterozoic snowball glaciations from Ir anomalies, *Science*, *308*, 239–242.
- Chylek, P., and J. Wong (1995), Effect of absorbing aerosols on global radiation budget, *Geophys. Res. Lett.*, *22*, 929–931.
- Curtius, J., et al. (2005), Observations of meteoric material and implications for aerosol nucleation in the winter Arctic lower stratosphere derived from in situ particle measurements, *Atmos. Chem. Phys.*, *5*, 3053–3069.
- Cziczo, D. J., D. S. Thomson, and D. M. Murphy (2001), Ablation, flux and atmospheric implications of meteors inferred from stratospheric aerosol, *Science*, *291*, 1772–1775.
- Forster, P. M. (1995), Modeling ultraviolet radiation at the Earth's surface. Part 1. The sensitivity of ultraviolet irradiances to atmospheric changes, *J. Appl. Meteorol.*, *34*, 2412–2425.
- Gabrielli, P., et al. (2004), Meteoric smoke fallout over the Holocene epoch revealed by iridium and platinum in Greenland ice, *Nature*, *432*, 1011–1014.
- Gerding, M., G. Baumgarten, U. Blum, J. P. Thayer, K. H. Fricke, R. Neuber, and J. Fiedler (2003), Observation of an unusual mid-stratospheric aerosol layer in the Arctic: possible sources and implications for polar vortex dynamics, *Ann. Geophys.*, *21*, 1057–1069.
- Heck, P. R., B. Schmitz, H. Baur, A. N. Halliday, and R. Wieler (2004), Fast delivery of meteorites to Earth after a major asteroid collision, *Nature*, *430*, 323–325.
- Henning, T. (1998), Chemistry and physics of cosmic nano- and micro-particles, *Chem. Soc. Rev.*, *27*, 315–321.
- Hoffman, P. H., A. J. Kaufman, G. P. Halverson, and D. P. Schrag (1998), A Neoproterozoic snowball Earth, *Science*, *281*, 1342–1346.
- Huang, T., et al. (1998), Description of SOCRATES—A chemical dynamical radiative two-dimensional model, *NCAR Tech. Note, NCAR/TN-440+EDD*, Natl. Cent. for Atmos. Res., Boulder, Colo.
- Hunten, D. M., R. P. Turco, and O. B. Toon (1980), Smoke and dust particles of meteoric origin in the mesosphere and stratosphere, *J. Atmos. Sci.*, *37*, 1342–1357.
- Jacobson, M. Z. (2005), *Fundamentals of Atmospheric Modeling*, 2nd ed., Cambridge Univ. Press, New York.
- Jäger, C., B. C. Il'in, T. Henning, H. Mutschke, D. Fabian, D. A. Semenov, and N. V. Voshchinnikov (2003), A database of optical constants of cosmic dust analogues, *J. Quant. Spectrosc. Radiat. Transfer*, *79*, 765–774. (Available at <http://www.astro.uni-jena.de/Laboratory/OCDDB/newsilicates.html>)
- Kasten, F. (1968), Falling speed of aerosol particles, *J. App. Meteorol.*, *7*, 944–947.
- Kirschvink, J. L. (1992), Late Proterozoic low-latitude global glaciation: The snowball Earth, in *The Proterozoic Biosphere*, edited by J. W. Schopf and C. Klein, pp. 51–52, Cambridge Univ. Press, New York.
- McKay, C. P., and G. E. Thomas (1978), Consequences of a past encounter of Earth with an interstellar cloud, *Geophys. Res. Lett.*, *5*, 215–218.
- Ossenkopf, V. (1991), Effective-medium theories for cosmic dust grains, *Astron. Astrophys.*, *251*, 210–219.
- Pavlov, A. A., O. B. Toon, A. K. Pavlov, J. Bally, and D. Pollard (2005), Passing through a giant molecular cloud: “Snowball” glaciations produced by interstellar dust, *Geophys. Res. Lett.*, *32*, L03705, doi:10.1029/2004GL021890.
- Plane, J. M. C. (2003), Atmospheric chemistry of meteoric metals, *Chem. Rev.*, *103*, 4963–4984.
- Plane, J. M. C. (2004), A time-resolved model of the mesospheric Na layer: Constraints on the meteor input function, *Atmos. Chem. Phys.*, *4*, 627–638.
- Rapp, M., and F.-J. Lübken (2001), Modelling of particle charging in the polar summer mesosphere: Part 1—General results, *J. Atmos. Sol. Terr. Phys.*, *63*, 759–770.
- Rapp, M., and G. E. Thomas (2006), Modeling the microphysics of mesospheric ice particles: Assessment of current capabilities and basic sensitivities, *J. Atmos. Sol. Terr. Phys.*, *68*, 715–744.
- Rietmeijer, F. J. M. (2002), Collected extraterrestrial materials: interplanetary dust particles, micrometeorites, meteorites and meteoritic dust, in *Meteors in the Earth's Atmosphere*, edited by E. Murad and I. P. Williams, pp. 215–245, Cambridge Univ. Press, New York.
- Saunders, R. W., and J. M. C. Plane (2006), A laboratory study of meteor smoke analogues: composition, optical properties and growth kinetics, *J. Atmos. Sol. Terr. Phys.*, *68*, 2182–2202.
- Schmitz, B., B. Peucker-Ehrenbrink, M. Lindström, and M. Tassinari (1997), Accretion rates of meteorites and cosmic dust in the early Ordovician, *Science*, *278*, 88–90.
- Yabushita, S., and A. J. Allen (1989), On the effect of accreted interstellar matter on the terrestrial environment, *Mon. Not. R. Astron. Soc.*, *238*, 1465–1478.

P. M. Forster, School of Earth and Environment, University of Leeds, Leeds LS2 9JT, UK. (p.forster@see.leeds.ac.uk)

J. M. C. Plane and R. W. Saunders, School of Chemistry, University of Leeds, Leeds LS2 9JT, UK. (j.m.c.plane@leeds.ac.uk; r.w.saunders@leeds.ac.uk)